COMPUTATIONAL RESEARCH PROGRESS IN APPLIED SCIENCE & ENGINEERING (CRPASE)

CRPASE: TRANSACTIONS OF MECHANICAL ENGINEERING

Journal homepage: http://www.crpase.com

CRPASE: Transactions of Mechanical Engineering, Vol. 06(03), 191-196, September 2020 ISSN 2423-4591

Research Article

Finite Element Analysis of an Aircraft Morphing Wing

Mehmet Akif Kaya*, Mostafa Ranjbar

Faculty of Engineering and Natural Sciences, Ankara Yildirim Beyazit University, Aankara, Turkey

Keywords

Morphing wing,
Aircraft,
Finite Element Analysis,
Wings Design.

Abstract

Aircraft wings are a compromise that allows the aircraft to fly at a range of flight conditions. Wings of the morphing type are meaningful advancements of the conventional structures as they are benefit to maneuverability and economy of aircrafts. Aims to demonstrate features of morphing wings' performance, this paper conducts a comprehensive Finite Element Analysis to a morphing wing after the object had been carefully designed. The deformation, strain energy, equivalent stress, and equivalent elastic strain of the morphing wing after applying a certain pressure are reached according to the constructed Finite Element model. Conclusion such as stress concentration point, maximum deformation, etc. of the morphing wing are suggested according to the analytic results.

1. Introduction

Air planes have played an important role in history since the first airplane was invented in 1903 [1, 2]. Developments in science and technology have led to more advanced air plane structures that offer high efficiency, lower cost, greater maneuver ability, the ability to cruise, and so forth [3, 4]. In recent years, the study of airplane wings has become a hot topic, with the particular interest in morphing wings [3-6]. Originally, morphing wings are inspired by birds, which have a large potential to improve the overall aircraft performances [7, 8]. Morphing aircraft are multi-role aircraft that change their external shape substantially to adapt to a changing mission environment during flight [8]. This creates superior system capabilities not possible without morphing shape changes. The objective of morphing activities is to develop high performance aircraft with wings designed to change shape and performance substantially during flight to create multiple-regime, aerodynamically-efficient, shape-changing aircraft [8-10]. Compared to conventional aircraft, morphing aircraft become more competitive as more mission tasks or roles are added to their requirements.

Morphing wing has been in aviation industry. Firstly, Wright brothers decided to use twist which is out of plane type of morphing wing, they used it to roll the aircraft and it worked [8, 11]. As years pass by many aeronautical engineers started getting interested in morphing wing concept and started to experiment, the problem they were facing was with the material which can be used efficiently and at low cost [8, 12]. In 1951 the aircraft X-5 was flown with variable sweep wing which could change its shape depending on speed and it was quite efficient and later on aircrafts such F14 and F111 were also using same design geometry and this time the material was using Titanium which was very strong and light material, it is being used still in aviation industry [13, 14]. Designers faced the problem of weight which still continues to be the problem for morphing wing aircraft but they did not let this issue to stop them so many designers designed morphing wing technology and applied into smaller scale in aircraft which included chord changing, leading and trailing edge changing, flaps changing one of the examples were F16 and F18 which uses leading edge changing morphing technology which is quite beneficial [14]. Latest and very successful example of morphing wing technology is Morphing Flap system which was made by Flexsys company for the Gulf Learjet [15-17]. Designers are continuing to find appropriate design of morphing wing which will be efficient in fuel, would be having less weight and at the same time less cost price [8, 17].

The current use of multiple aerodynamic devices (such as flaps and slats) represents a simplification of the general idea

* Corresponding Author: Mostafa Ranjbar
E-mail address: mranjbar@ybu.edu.tr

Received: 12 June 2020; Revised: 10 July 2020; Accepted: 20 July 2020

Please cite this article as: M.A. Kaya, M. Ranjbar, Finite Element Analysis of an Aircraft Morphing Wing, Computational Research Progress in Applied Science & Engineering, CRPASE: Transactions of Mechanical Engineering 6 (2020) 191–196.

behind morphing. Traditional control systems (with fixed geometry and/or location) give high aerodynamic performance over a fixed range and for a limited set of flight conditions [17, 18]. Outside of this range, these traditional systems can be neutral or negatively influence the aerodynamics and hence often give lower efficiency [17, 19]. Conventional hinged mechanisms are effective in controlling the airflow, but they are not efficient, as the hinges and other junctions usually create discontinuities in the surface, resulting in unwanted fluid dynamic phenomena. Since 1920, airplanes have used devices that can increase the lift during landing and takeoff [20]. Increases in aircraft weight, cruise speed, and increases in the wing structural stiffness to avoid multiple aero-elastic phenomena (divergence, flutter, etc.) have led to the use of discrete control surfaces such as ailerons and flaps in place of wing twist [8, 17]. Researchers, gradually, seriously revisited concepts of variable wing shape. Most of this research was based on two concepts, namely the active control of the curvature along the wingspan and the implementation of flexible wings, able to exploit the aero-elastic forces to obtain the desired deformations (wing shapes) [21. 22].

Civilian airplanes consume large amounts of fuel during a flight [23, 24]. The weight of fuel accounts for more than 30% of the airplane's total weight [17, 24]. A morphing wing with a variable camber trailing edge reduces fuel consumption by at least 5% and increases the lift coefficient from 0.08 to 0.4 [8, 17, 23, 24].

Changing the wing shape or geometry is not new. Historically, morphing solutions always led to penalties in terms of cost, complexity, or weight, although in certain circumstances, these were overcome by system-level benefits [25]. The current trend for highly efficient and 'green' aircraft makes such compromises less acceptable, calling for innovative morphing designs able to provide more benefits and fewer drawbacks [26]. Recent developments in 'smart' materials may overcome the limitations and enhance the benefits from existing design solutions. The challenge is to design a structure that is capable of withstanding the prescribed loads, but is also able to change its shape.

Under the condition that the performance of morphing wings of aircraft is limited, this paper presents a detailed feature analysis of a designed morphing wing by using Finite Element Analysis (FEA) to demonstrate the corresponding mechanical properties of the morphing wing. The reminder of this paper is arranged as follows. Section 2 presents some basic concepts associated with morphing wings. Section 3 introduced the morphing wing model of this study. The FEA is implemented in Section 4. Conclusion of this study is provided in Section 5.

2. Basic Concepts of Morphing Wing

2.1. Wing Profile

A typical wing profile is displayed in Figure 1. In aeronautics, the thickness ratio compares the maximum vertical thickness of a wing to its chord. It is a key measure of the performance of a wing planform when it is operating at transonic speeds. To be specific, in civil aircraft, it is possible to come across wing profiles with various thickness ratios between 8-9% and 18-20% depending on the duty speed of the plane. Typically, thickness ratio of wing profile can be divided into thin profile (thickness ratio less than 0.1), medium thickness profile (0.1-0.14), and thick profile (over 0.14) [27].

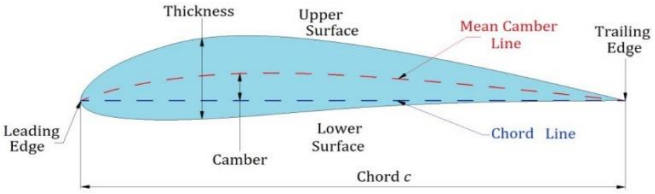

Figure 1. Typical wing profile geometry

The maximum thickness point is usually between 30% and 60% of the vet. In some old profiles it is possible to see that this point is at 25% of the vet. In some exceptional profiles, the maximum thickness point can be found lower than 60% of the veterinarian. Wing profiles can be symmetrical or humped. Symmetrical profiles are not used in aircraft wings, rather, they are used on vertical and horizontal tail surfaces, in the connecting elements between the wings of biplane aircraft, in the bodywork of the elements that create parasitic resistance on the aircraft such as landing gear and so on. To be comparable, humpbacks between 0 and 5% are found on the airplane wings. It is possible to see more humped profiles in turbines and compressors.

Overall, 2 force components (Carriage and Drag) and 1 moment component (Pitching) affect the wing profile. It is possible to achieve transport and drag by integrating the pressure distribution across the surface. Although it seems possible to find drag by integrating pressure and friction distributions across the surface, this is generally very difficult. Therefore, drag is obtained by measuring the loss of momentum. Although the performance of the wing profile determines the Transport and Drag forces and the Pitching moment, it is often concerned with these coefficients instead of these force and moment components. In general, the aerodynamic coefficients of the wing profile depend primarily on the geometric shape and angle of attack of the profile, and then on the Reynolds and Mach numbers.

2.2. Angle of Attack

In fluid dynamics, angle of attack is the angle between a reference line on a body (often the chord line of an airfoil) and the vector representing the relative motion between the body and the fluid through which it is moving [28]. Angle of attack is the angle between the body's reference line and the oncoming flow. This article focuses on the most common application, the angle of attack of a wing or airfoil moving through air.

In aerodynamics, angle of attack specifies the angle between the chord line of the wing of a fixed-wing aircraft and the vector representing the relative motion between the aircraft and the atmosphere. Since a wing can have twist, a chord line of the whole wing may not be definable, so an alternate reference line is simply defined. Often, the chord line of the root of the wing is chosen as the reference line. Another choice is to use a horizontal line on the fuselage as the reference line (also as the longitudinal axis).

Low angle of attack results in sufficient buoyancy, while an over-high angle of attack causes turbulence and may even cause the blade to break in the air stream. Therefore, designers must ensure that the angle of attack is at optimal levels (15 degrees generally).

The critical angle of attack is the angle of attack which produces the maximum lift coefficient. This is also called the "stall angle of attack". Below the critical angle of attack, as the angle of attack decreases, the lift coefficient decreases. Conversely, above the critical angle of attack, as the angle of attack increases, the air begins to flow less smoothly over the upper surface of the airfoil and begins to separate from the upper surface. On most airfoil shapes, as the angle of attack increases, the upper surface separation point of the flow moves from the trailing edge towards the leading edge. At the critical angle of attack, upper surface flow is more separated and the airfoil or wing is producing its maximum lift coefficient. As the angle of attack increases further, the upper surface flow becomes more fully separated and the lift coefficient reduces further.

Above this critical angle of attack, the aircraft is said to be in a stall. A fixed- wing aircraft is stalled at or above the critical angle of attack rather than at or below a particular airspeed. The airspeed at which the aircraft stalls varies with the weight of the aircraft, the load factor, the center of gravity of the aircraft and other factors. However, the aircraft always stalls at the same critical angle of attack. The critical or stalling angle of attack is typically around 15-20 degrees for many airfoils.

3. Morphing Wing Design

The design of the morphing wing follows the predetermined steps [29-31]:

(1) Model determination. The NASA sc(2)-0714 model was selected to be the an aircraft model of this study (two Dimensional (2D) coordinates of which is available at http://airfoiltools.com/), see Figure 2.

(2) Extend 2D coordinates to 3D view. Transfer the 2D coordinates to Microsoft EXCEL and then add the z coordinates as zero to obtain the 3D view.

(3) 3D model establishments. Save values in Step (2) text form to transfer SOLIDWORKS software and configure the 3D model of the morphing wing.

The morphing wing s divided into two different parts: fixed part (part 1) and morphing part (part 2).

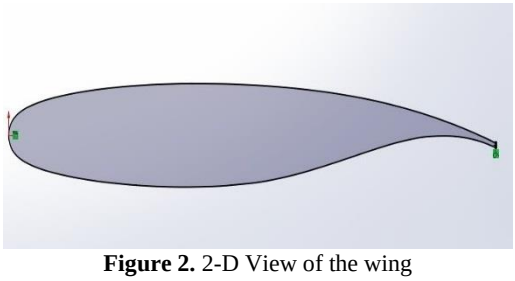

Figure 2. 2-D View of the wing

4. Finite Element Analysis (FEA)

To create buoyancy, the surface area of the upper part of the morphing wing is larger than the lower side. Due to this difference, a high-pressure area occurs in the lower section and a low-pressure area in the upper section. Thanks to this pressure difference, the buoyancy can be obtained from the air.

To observe the mechanical reaction of the morphing wing against this pressure difference, we create a high-pressure area at the bottom of the morphing wing and apply it to the wing through the ANSYS program. The aim in doing this is to observe the stress, resistance, and deformation changes that may occur on the wing and to determine the critical points on the morphing wing model.

The analytic steps using ANSYS for analysis of the morphing wing as follows [32-36]:

(1) Save and then transfer the morphing wing model form SOLIDWORKS to ANSYS.

(2) Parameter definition. Define geometry, material (Aluminum), etc. of the morphing wing in the finite element model in the ANSYS software.

(3) Meshing: Mesh, elaborately, the finite element model in the ANSYS software.

(4) Analysis implementation. Conduct analysis and monitor outcomes as deformation, stress, strain, and energy change.

The deformation, strain energy, equivalent stress, and equivalent elastic strain of the morphing wing after applying 1 MPa pressure is displayed in Figures 3-6, respectively.

As seen from the Figure 3, after applying pressure, maximum deformation occurs at the end points of our wing. Since these parts are the most distant parts of our wing from the main body, as a result of the strength calculations, the most force occurs in the extreme regions. Therefore, deformation in the extreme regions is more. In contrast, as the surface area, the least amount of expansion occurs in the parts of the wing welded to the main body. The reason for this is that the momentum acting on those regions is less. Therefore, minimum deformation occurs in areas close to the body.

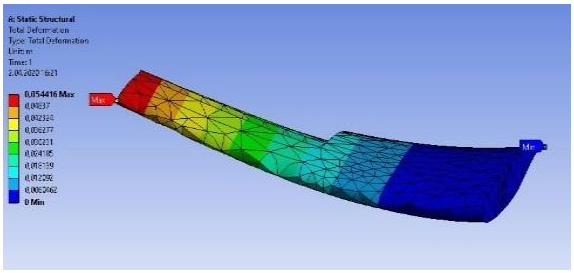

Figure 3. Deformation of morphing wing after 1 MPa pressure applied

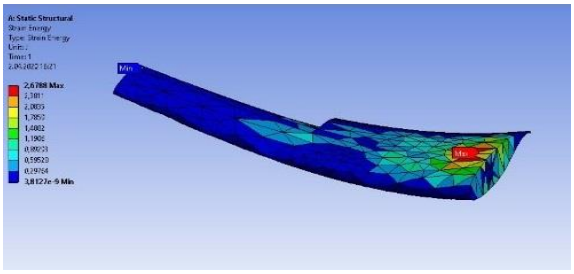

Figure 4. Strain energy distribution of the morphing wing after 1 MPa pressure applied

The total shear energy changes occur mostly in the upper part of the morphing wing, closest to the body. The slip occurs perpendicular to the lateral axis. And it tends to

happen in fixed sections with the most reaction force. Since less energy is dissipated to the tip of the morphing wing, less compensating force is generated at the tip. And this results in less strain energy occur at the ends.

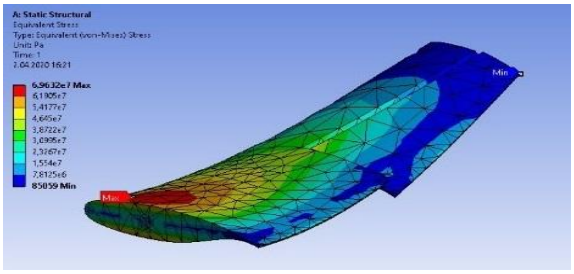

Figure 5. Equivalent stress distribution of the morphing wing after 1 MPa pressure applied

As shown in the Figure 5, the maximum equivalent stress occurs in the parts of the upper part of the wing closest to the main body. The pressure acting from below causes the wing to bend upwards. And this causes the wing to squeeze the upper parts and the lower parts to elongate. For this reason, the maximum equivalent stress occurs in these regions. Since the opposite is true at the ends, the minimum equivalent stresses are obtained at the ends as shown in the Figure 5.

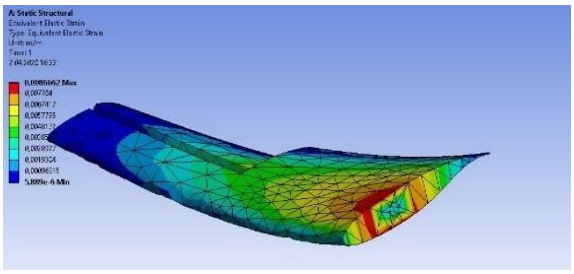

Figure 6. Equivalent elastic strain of the morphing wing after 1 MPa pressure applied

As shown in the Figure 6, the maximum equivalent elastic strain is seen in the center and near the part of the wing closest to the main body. Since the morphing wing is welded to the main body, the maximum elastic strain tendency is observed in the center and the periphery of the wing close to the body. However, since the ends of the morphing wing are far from the welded part, the amount of energy to be generated in those parts is minimum. Therefore, equivalent elastic slip occurs in the minimum amount in the end parts of the plane where it can be seen from the shape.

As can be seen from all these analyzes, different regions of the wing gave various reactions to different types of analysis. And basically, it is concluded that the critical points are the tip of our wing and the part welded to the body. Because energy and deformation changes took place in these regions with maximum and minimum. These analyzes are very important. Because the evaluation and scoring of any product designed is done by looking at these analyzes. And if necessary, the design can be redone in some projects. As a result, these analyzes are very important results that shed light on us.

5. Conclusions

Wings of the morphing type are meaningful advancements of the conventional structures as they are benefit to maneuverability and economy of aircrafts. This paper conducts a comprehensive Finite Element Analysis to a morphing wing after the object had been carefully designed. The following conclusions are achieved based on the outcomes of the analysis:

(1) Maximum deformation occurs at the end points of the morphing wing as these parts are the most distant parts from the main body. The expansion of the parts of the wing welded to the main body is minor.

(2) The total shear energy changes occur mostly in the upper part of the morphing wing, closest to the body.

(3) The maximum equivalent stress occurs in the parts of the upper part of the wing closest to the main body.

(4) The maximum equivalent elastic strain is in the center of the wing and at the meanwhile the equivalent elastic slip occurs in the minimum amount in the end parts of the plane. As a direction for future work we will consider applying some techniques such as but not limited to [36-51].

Conflict of Interest Statement

The authors declare no conflict of interest.

References

[1] U. Iemma, F.P. Vitagliano, F. Centracchio, A multi-objective design optimisation of eco-friendly aircraft: the impact of noise fees on airplanes sustainable development, International Journal of Sustainable Engineering 11 (2018) 122–134.

[2] A. Bejan, J.D. Charles, S. Lorente, The evolution of airplanes, Journal of Applied Physics 116 (2014) 044901.

[3] A.Y.N. Sofla, S.A. Meguid, K.T. Tan, W.K. Yeo, Shape morphing of aircraft wing: Status and challenges, Materials & Design 31(2010) 1284–1292.

[4] M. Montemurro, A. Vincenti, P. Vannucci, A two-level procedure for the global optimum design of composite modular structures-application to the design of an aircraft wing, Journal of Optimization Theory and Applications 155(2012) 24–53.

[5] J.W. Kruyt, G.F. van Heijst, D. L. Altshuler, D. Lentink, Power reduction and the radial limit of stall delay in revolving wings of different aspect ratio, Journal of the Royal Society Interface 12 (2015) 20150051.

[6] E. Oktay, H.U. Akay, O. Merttopcuoglu, Parallelized structural topology optimization and CFD coupling for design of aircraft wing structures, Computers & Fluids 49 (2011) 141–145.

[7] A.M. Wickenheiser, E. Garcia, Aerodynamic modeling of morphing wings using an extended lifting-line analysis, Journal of Aircraft 44 (2007) 10–16.

[8] D. Li, S. Zhao, A. Da Ronch, J. Xiang, J. Drofelnik, Y. Li, L. Zhang, Y. Wu, M. Kintscher, H.P. Monner, A. Rudenko, S. Guo, W. Yin, J. Kirn, S. Storm, R. De Breuker, A review of modelling and analysis of morphing wings, Progress in Aerospace Sciences 100 (2018) 46-62.

[9] N. Tsushima, T. Yokozeki, W. Su, H. Arizono, Geometrically nonlinear static aeroelastic analysis of composite morphing wing with corrugated structures, Aerospace Science and Technology 88 (2019) 244–257.

[10] G. Molinari, A.F. Arrieta, M. Guillaume, P. Ermanni, Aerostructural performance of distributed compliance morphing wings: wind tunnel and flight testing, AIAA journal 54 (2016) 3859–3871.

[11] J.M. Weaver-Rosen, P.B. Leal, D.J. Hartl, R.J. Malak, Parametric optimization for morphing structures design: application to morphing wings adapting to changing flight

conditions, Structural and Multidisciplinary Optimization, (2020) 1–13.
[12] A. De Gaspari, S. Ricci, A two-level approach for the optimal design of morphing wings based on compliant structures, Journal of Intelligent Material Systems and Structures 22 (2011) 1091–1111.
[13] S. Chen, K. Yue, B. Hu, R. Guo, Numerical simulation on the radar cross section of variable-sweep wing aircraft, Journal of Aerospace Technology and Management, 7 (2015) 170-178.
[14] Z. Min, V.K. Kien, L.J. Richard, Aircraft morphing wing concepts with radical geometry change, The IES Journal Part A: Civil & Structural Engineering 3 (2010) 188–195.
[15] S. Daynes, P.M. Weaver, A morphing trailing edge device for a wind turbine, Journal of Intelligent Material Systems and Structures 23 (2012) 691–701.
[16] A.S. Panesar, P.M. Weaver, Optimisation of blended bistable laminates for a morphing flap, Composite Structures 94 (2012) 3092–3105.
[17] T.A. Weisshaar, Morphing aircraft systems: historical perspectives and future challenges, Journal of aircraft 50 (2013) 337-353.
[18] R.M. Ajaj, C.S. Beaverstock, M. I. Friswell, Morphing aircraft: The need for a new design philosophy, Aerospace Science and Technology 49 (2016) 154–166.
[19] S. Vasista, F. Nolte, H.P. Monner, P. Horst, M. Burnazzi, Three-dimensional design of a large-displacement morphing wing droop nose device, Journal of intelligent material systems and structures 29 (2018) 3222–3241.
[20] J. Katz, S. Byrne, R. Hahl, Stall resistance features of lifting-body airplane configurations, Journal of aircraft 36 (1999) 471-474.
[21] P. Bourdin, A. Gatto, M.I. Friswell, Aircraft control via variable cant-angle winglets, Journal of Aircraft 45 (2008) 414–423.
[22] G. Reich, B. Sanders, Introduction to morphing aircraft research, Journal of aircraft 44 (2007) 1059–1059.
[23] X. Zhu, Z. Guo, Z. Hou, Solar-powered airplanes: A historical perspective and future challenges, Progress in aerospace sciences 71 (2014) 36-53.
[24] D. Chen, J. Sun, Fuel and emission reduction assessment for civil aircraft engine fleet on-wing washing, Transportation Research Part D: Transport and Environment 65 (2018) 324–331.
[25] U. Fasel, D. Keidel, G. Molinari, P. Ermanni, Aerostructural optimization of a morphing wing for airborne wind energy applications, Smart Materials and Structures 26 (2017) 095043.
[26] R.E. Bartels, C.J. Funk, R.C. Scott, Limit-Cycle Oscillation of the Subsonic Ultra-Green Aircraft Research Truss-Braced Wing Aeroelastic Model, Journal of Aircraft 54 (2017) 1605–1613.
[27] A. Silverstein, S. Katzoff, A simplified method for determining wing profile drag in flight, Journal of the Aeronautical Sciences 7 (1940) 295–301.
[28] N. Tajuddin, S. Mat, M. Said, S. Mansor, Flow characteristic of blunt-edged delta wing at high angle of attack, Journal of Advanced Research in Fluid Mechanics and Thermal Sciences 39 (2017) 17–25.
[29] M. Arena, A. Concilio, R. Pecora, Aero-servo-elastic design of a morphing wing trailing edge system for enhanced cruise performance, Aerospace Science and Technology 86 (2019) 215-235.
[30] A. Sari, H. Fatahian, E. Fatahian, Numerical Investigation of Heat Transfer of Flow Over the Cylinder with High Conductivity Fins, Computational Research Progress in Applied Science & Engineering 3 (2017) 85–95.
[31] N. Tsushima, T. Yokozeki, W. Su, H. Arizono, Geometrically nonlinear static aeroelastic analysis of composite morphing wing with corrugated structures, Aerospace Science and Technology 88 (2019) 244–257.
[32] H. Li, H.Z. Huang, Y.F. Li, J. Zhou, J. Mi, Physics of failure-based reliability prediction of turbine blades using multi-source information fusion, Applied Soft Computing 72 (2018) 624-635.
[33] A.A.R. Aliloa, G. Bhatt, FEM Based Study on Optimum Design of Geometry for RC Rectangular Silo Bearing Extreme Asymmetrical Static Loads, Computational Research Progress in Applied Science & Engineering 04 (2018) 77–82.
[34] S.T. Jouybari, G.A. Shafabakhsh, Finite Element Investigation of Load Transfer Efficiency in Jointed Plain Concrete Pavements, Computational Research Progress in Applied Science & Engineering 3 (2017) 91–96.
[35] B.P. Shetty, S. Reddy, R.K. Mishra, Finite element analysis of an aircraft wing leading edge made of glare material for structural integrity, Journal of Failure Analysis and Prevention 17 (2017) 948-954.
[36] N. A. Golilarz, N. Robert, J. Addeh, A. Salehpour, Translation invariant wavelet based noise reduction using a new smooth nonlinear improved thresholding function, Computational Research Progress in Applied Science & Engineering 3 (2017) 104–108.
[37] N. A. Golilarz, N. Robert, J. Addeh, Survey of image de-noising using wavelet transform combined with thresholding functions, Computational Research Progress in Applied Science & Engineering 3 (2017) 132–135.
[38] N. A. Golilarz, H. Demirel, Thresholding neural network (TNN) based noise reduction with a new improved thresholding function, Computational Research Progress in Applied Science & Engineering 3 (2017) 81–84.
[39] A. Addeh, A. Khormali, N. A. Golilarz, Control chart pattern recognition using RBF neural network with new training algorithm and pracrical features, ISA Transactions 79 (2018) 202–216.
[40] N. A. Golilarz, A. Addeh, H. Gao, L. Ali, A. M. Roshandeh, H. M. Munir, R. Khan, A new automatic method for control chart patterns recognition based on ConvNet and harris hawks meta heuristic optimization algorithm, IEEE Access 7 (2019) 149398–149405.
[41] L. Ali, S. Khan, N. A. Golilarz, Y. Imrana, I. Qasim, A. Noor, R. Nour, A Feature-Driven Decision Support System for Heart Failure Prediction Based on χ 2 Statistical Model and Gaussian Naive Bayes, Computational and Mathematical Methods in Medicine (2019) 1–8.
[42] R. Khan, X. Zhang, R. Kumar, A. Sharif, N. A. Golilarz, M. Alazab, An Adaptive Multi-Layer Botnet Detection Technique Using Machine Learning Classifiers, Applied Sciences 9 (2019).
[43] L. Ali, C. Zhu, N. A. Golilarz**,** A. Javeed, M. Zhou, Y Liu, Reliable Parkinson's Disease Detection by Analyzing Handwritten Drawings: Construction of an Unbiased Cascaded Learning System based on Feature Selection and Adaptive Boosting Model, IEEE Access 7 (2019) 116480–116489.
[44] L. Ali, A. Niamat, J. A. Khan, N. A. Golilarz, X. Xingzhong, A. Noor, R. Nour, S. A. Chan Bukhari, An Optimized Stacked Support Vector Machines Based Expert System for the Effective Prediction of Heart Disease, IEEE Access 7 (2019) 54007–54014.
[45] N. A. Golilarz, H. Gao, H. Demirel, Satellite Image De-noising with Harris Hawks Meta Heuristic Optimization Algorithm and Improved Adaptive Generalized Gaussian Distribution Threshold Function, IEEE Access 7 (2019) 57459 - 57468.
[46] H. M. Munir, R. Ghannam, H. Li, T. Younas, N. A. Golilarz, M. Hassan, A. Siddique, Control of Distributed Generators and Direct Harmonic Voltage Controlled Active Power Filters for Accurate Current Sharing and Power Quality Improvement in Islanded Microgrids, Inventions 4, (2019).

[47] L. Ali, I. Wajahat, N. A. Golilarz, F. Keshtkar, and S. A. C. Bukhari, Lda-ga–svm: improved hepatocellular carcinoma prediction throughdimensionality reduction and genetically optimized support vector machine, Neural Computing and Applications (2020) 1–10.

[48] H. Chen, C. Yang, A. A. Heidari, X. Zhao, An efficient double adaptive random spare reinforced whale optimization algorithm, Expert Systems with Applications 154 (2020) 113018.

[49] I. Aljarah, M. Mafarja, A. A. Heidari, H. Faris, S. Mirjalili, Clustering analysis using a novel locality-informed grey wolf-inspired clustering approach, Knowledge and Information Systems 62 (2019) 507–539.

[50] H. Chen, A. A. Heidari, X. Zhao, L. Zhang, H. Chen, Advanced orthogonal learning-driven multi-swarm sine cosine optimization: Framework and case studies, Expert Systems with Applications 144 (2020) 113113.

[51] Z. Xu, Z. Hu, A. A. Heidari, M. Wang, X. Zhao, H. Chen, X. Cai, Orthogonally-designed adapted grasshopper optimization: A comprehensive analysis, Expert Systems with Applications 150 (2020) 113282.